Dalton Transactions

RSC Publishing

PAPER

View Article Online
View Journal | View Issue

Cite this: *Dalton Trans.*, 2013, **42**, 10515

Tungstic acid functionalized mesoporous SBA-15: A novel heterogeneous catalyst for facile one-pot synthesis of 2-amino-4*H*-chromenes in aqueous medium

Sudipta K. Kundu, John Mondal and Asim Bhaumik*

Received 10th April 2013,
Accepted 13th May 2013

DOI: 10.1039/c3dt50947h

www.rsc.org/dalton

A new highly ordered mesoporous tungstic acid functionalized SBA-15, TAFMC-1 has been synthesized *via* post-synthesis modification of mesoporous SBA-15 with (3-chloropropyl) triethoxysilane followed by substitution reaction of chlorine atom of the 3-chloropropyl group by tungstic acid group under refluxing conditions in *n*-hexane. The tungstic acid functionalized mesoporous silica material has been characterized by using small angle powder X-ray diffraction, N_2 sorption, HR-TEM, FE-SEM, FT-IR and solid state MAS NMR studies. TAFMC-1 catalyzes the facile one-pot catalytic three-component condensation reaction of resorcinol, aromatic aldehyde and malononitrile for the synthesis of a diverse range of 2-amino-4*H*-chromenes in aqueous medium. This heterogeneous catalyst can be recycled very efficiently for six consecutive reaction cycles without significant loss of catalytic activity.

Introduction

Recently, an increasing attention has been focused for the development of new synthetic routes in chemical processes employing nontoxic solvent, reagents and catalysts. In order to execute the reactions under nontoxic conditions the multicomponent reaction (MCR) strategy has been adopted by researchers.[1] The simplicity of the one-pot procedure, accessibility of a variety of compounds, conducting reaction without isolation of intermediate, reduction of time and energy are the major advantages of the MCR type reactions compared with the conventional reaction procedures.[2] Because of these advantages, multicomponent coupling reactions are preferred to tune the synthetic reaction steps for combinatorial synthesis.[3] Various heterocyclic compounds such as benzopyrans, benzoxanthene, benzochromene can be developed by applying this one-pot multicomponent reaction strategy. Benzochromenes are the most important class of biologically active heterocyclic compounds which have attracted an emerging interest in recent research areas due to their antimicrobial,[4] anti-inflammatory,[5] antibacterial,[6] antiviral[7] and anticancer[8] activities. In addition, they can be employed as the building blocks of several human drugs, which are used for the treatment of neurodegenerative diseases, including Alzheimer's disease, amyotrophic lateral sclerosis, Huntington's disease, Parkinson's disease, AIDS associated dementia and Down's syndrome as well as for the treatment of schizophrenia and myoclonus.[9] Synthesis of these important class of compounds have made significant impact in the field of cosmetics, pigments and potential biodegradable agrochemicals.[10]

Owing to their versatile applications, researchers are keener to synthesize amino chromene derivative over various Lewis acid and base catalysts such as NaOH,[11] K_2CO_3,[12] MgO,[13] $TiCl_4$,[14] $InCl_3$,[15] heteropolyacid and Et_3N.[16] Although, most of these catalytic methods showed high activity and selectivity, these catalysts are homogeneous in nature. The main problem traditionally associated with these homogeneous catalysts includes separation of the catalyst from the reaction mixture after the reaction. Reusability and recovery of the most expensive catalysts plays a decisive role for the sustainable development of any catalytic procedure. Catalyst separation has become the most influential, powerful and practical technique in the field of heterogeneous catalyst and separation of the active catalysts that are very important to recycle/reuse are hugely acknowledged in the chemical industry. So the development of heterogeneous catalysts that are employed to perform the most efficient and economically feasible catalytic processes synthesized through the heterogenisation of homogeneous catalytic sites on the solid supports is highly desirable.

Recently mesoporous material has witnessed a remarkable growth in academia and industry in this context. Exceptionally high surface area, tunable pore size distribution, high

Department of Materials Science, Indian Association for the Cultivation of Science, Jadavpur 700 032, India. E-mail: msab@iacs.res.in

hydrothermal and mechanical stability make them a potential candidate in the field of heterogeneous catalysis.[17] Mesoporous materials are hugely acknowledged as a platform for solid support, where various active sites can be effectively anchored. The size, shape and connectivity of the existing pores can be tuned in the organically functionalized mesoporous materials *via* some chemical reactions, where the metal atom or active sites can be covalently anchored with the functional groups present at the surface of the catalysts.[18] Thus, considerable attention has been paid to design the organic–inorganic hybrid mesoporous silica, where the active metal and catalytic sites can be covalently grafted with the organic functional groups so that no leaching could take place during the course of the reaction. Recently, we have developed triazine functionalized mesoporous organocatalyst (TFMO-1) which exhibited excellent catalytic activity in one-pot three component condensation reaction under solvent-free conditions to develop 2-amino-4*H*-chromene.[19]

Herein, we wish to report the synthesis of a robust and non-air sensitive tungstic acid functionalized mesoporous SBA-15 silica by post-grafting approach over mesoporous SBA-15 material. The catalyst has been developed by the surface modification technique of mesoporous SBA-15 silica by using (3-chloropropyl)triethoxysilane in toluene solvent. Then the chloro group has been substituted by a substitution reaction using sodium tungstate in *n*-hexane solvent. The tungstic acid functionalized SBA-15 heterogeneous catalyst has been thoroughly characterized by XRD, FT-IR, HRTEM, FE SEM, N_2 sorption, ^{13}C and ^{29}Si solid state MAS NMR studies. The catalyst showed excellent catalytic activity for performing one-pot three component condensation reaction of resorcinol, malononitrile and aromatic aldehyde in aqueous medium for the synthesis of a diverse range of 2-amino-4*H*-chromene derivatives in very high yields (80–88%).

Experimental section

Synthesis of tungstic acid functionalized mesoporous SBA-15 (TAFMC-1)

Synthesis of mesoporous SBA-15. In a typical synthesis, 2.0 g of P123 was dissolved in 60 mL of 2.0 M aqueous HCl and 15.0 g of distilled water under stirring at room temperature. Then 4.25 g of tetraethyl orthosilicate (TEOS) was added dropwise to the solution of P123 in acid media at 40 °C. After TEOS was added, the mixture was stirred for 24 h and then transferred into a Teflon-lined autoclave and kept at 100 °C for another 24 h. Finally the solid product was recovered by filtration, washed with distilled water, and air-dried. The template was removed by calcination of the sample at 500 °C in air for 5 h to get the final product SBA-15.

General procedure for the synthesis of 3-chloropropyl functionalized SBA-15. 0.2 g calcined SBA-15 in 15 mL dry toluene was placed in a 50 mL round bottom flask. Then 0.6 mmol (0.144 g) (3-chloropropyl)triethoxysilane taken in 5 mL dry toluene was added dropwise to the dispersed SBA-15 solution under continuous stirring. Then it was refluxed for 24 h under nitrogen atmosphere. After completion of the reaction, the reaction mixture was allowed to cool at room temperature. Then it was filtered and washed thoroughly with toluene (10 mL), dichloromethane (10 mL) and diethylether (10 mL), respectively. The white colored sample was dried at room temperature.

Synthesis of TAFMC-1. Tungstic acid functionalized SBA-15 (TAFMC-1) was prepared by reaction with SBA-15-Cl and sodium tungstate dihydrate. 0.5 g of SBA-15-Cl in 15 mL *n*-hexane was placed in a 50 mL round bottom flask. Then 0.658 g of sodium tungstate dihydrate was added to the dispersed SBA-15-Cl solution and then it was refluxed for 12 h under a nitrogen atmosphere. After completion of reaction it was cooled to room temperature and filtered through suction followed by washing thoroughly with *n*-hexane (10 mL) and distilled water (10 mL), respectively. The sample was dried and then stirred in the presence of 15 mL aqueous HCl medium so that the pH of the solution comes down to *ca.* 4.0 in 1 h (Scheme 1). Finally the mixture was filtered, washed with distilled water and dried at room temperature.

General procedure for the synthesis of 2-amino-4*H*-chromenes. A mixture of aromatic aldehyde (1 mmol), malononitrile (1 mmol, 66 mg), resorcinol (1 mmol, 110 mg) and catalyst TAFMC-1 (30 mg) in water was refluxed in an oil bath for an appropriate period of time. After completion of reaction (monitored by TLC), the reaction mixture was allowed to cool to room temperature and 5 mL ethyl acetate was poured into the reaction mixture and then it was stirred for 30 min at room temperature. The catalyst was separated by filtration and it was washed with ethyl acetate by several times. The filtrate was washed with water (3 × 30 mL) and then dried over anhydrous Na_2SO_4 and evaporated. The crude product was recrystallized from ethanol to afford pure product.

Instrumentation. Powder X-ray diffraction patterns of SBA-15, SBA-15-Cl and TAFMC-1 samples were recorded on a Bruker D-8 Advance SWAX diffractometer operated at a voltage of 40 kV and a current of 40 mA and calibrated with a standard silicon sample, using Ni-filtered Cu-Kα (λ = 0.15406 nm). FT-IR

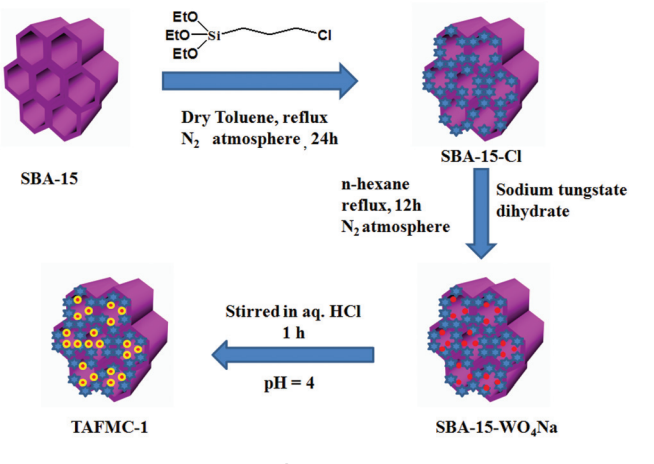

Scheme 1

spectra of the samples were recorded using a Nicolet MAGNA FT-IR 750 spectrometer series II. N_2 adsorption/desorption isotherms were obtained by using a Beckman coulter SA 3100 surface area analyzer at 77 K. JEOL JEM 6700F field emission scanning electron microscope (FE SEM) was used for the determination of morphology of powder samples. The pore structure was visualized by using a JEOL JEM 2010 high resolution transmission electron microscope (HR TEM) operated at an accelerating voltage of 200 kV. ^{1}H and ^{13}C NMR (solution) experiments were carried out on a Bruker DPX-300 NMR spectrometer. The solid state MAS NMR spectra of the samples were taken in a 500 MHz Bruker Avance II spectrometer.

^{1}H and ^{13}C NMR chemical shifts for different 2-amino-4*H*-chromene products

2-Amino-3-cyano-7-hydroxy-4-(4-phenyl)-4*H*-chromene (Table 1, entry 1, 4a). Yellow solid: ^{1}H NMR (500 MHz, DMSO-d_6) δ 9.69 (s, 1H), 7.29–7.31 (m, 2H), 7.16–7.21 (m, 3H), 6.85 (s, 2H), 6.79–6.81 (m, 1H), 6.47–6.49 (d, 1H), 6.41 (s, 1H), 4.61 (s, 1H); ^{13}C NMR (500 MHz, DMSO-d_6) δ 56.97, 102.81, 113.00, 114.38, 121.23, 127.24, 127.98, 129.19, 130.51, 146.97, 149.50, 157.70, 160.88.

2-Amino-3-cyano-7-hydroxy-4-(4-methylphenyl)-4*H*-chromene (Table 1, entry 2, 4b). Yellow solid: ^{13}C NMR (300 MHz, DMSO-d_6) δ 21.30, 57.01, 102.72, 112.91, 114.49, 121.26, 127.89, 129.04, 129.71, 130.77, 146.28, 149.39, 157.59, 160.74.

2-Amino-3-cyano-7-hydroxy-4-(4-fluorophenyl)-4*H*-chromene (Table 1, entry 3, 4c). Yellow solid: ^{1}H NMR (500 MHz, DMSO-d_6) δ 9.69 (s, 1H), 7.17–7.20 (m, 2H), 7.07–7.13 (m, 2H), 6.89 (s, 2H), 6.76–6.78 (d, 1H), 6.47–6.49 (m, 1H), 6.40 (s, 1H), 4.65 (s, 1H); ^{13}C NMR (500 MHz, DMSO-d_6) δ 56.20, 102.18, 112.43, 113.52, 115.12, 115.40, 120.52, 129.27, 129.86, 142.55, 148.80, 157.13, 160.18.

2-Amino-3-cyano-7-hydroxy-4-(4-chlorophenyl)-4*H*-chromene (Table 1, entry 4, 4d). Yellow solid: ^{1}H NMR (300 MHz, DMSO-d_6) δ 9.71 (s, 1H), 7.35–7.37 (d, 2H), 7.18–7.19 (d, 2H), 6.89 (s, 2H), 6.77–6.79 (d, 1H), 6.48–6.50 (d, 1H), 6.41 (s, 1H), 4.66 (s, 1H); ^{13}C NMR (300 MHz, DMSO-d_6) δ 56.45, 102.81, 113.05, 113.77, 121.06, 129.13, 129.85, 130.46, 131.81, 145.89, 149.40, 157.79, 160.82.

2-Amino-3-cyano-7-hydroxy-4-(4-bromophenyl)-4*H*-chromene (Table 1, entry 5, 4e). Yellow solid: ^{1}H NMR (500 MHz, DMSO-d_6) δ 9.72 (b, 1H), 7.46–7.51 (m, 2H), 7.12–7.14 (m, 2H), 6.90 (s, 2H), 6.77–6.79 (d, 1H, J = 10 Hz), 6.48–6.50 (m, 1H), 6.41 (s, 1H), 4.65 (s, 1H); ^{13}C NMR (500 MHz, DMSO-d_6) δ 56.38, 102.78, 113.03, 113.65, 120.26, 121.00, 130.20, 130.42, 132.01, 146.27, 149.37, 157.78, 160.79.

2-Amino-3-cyano-7-hydroxy-4-(2-bromophenyl)-4*H*-chromene (Table 1, entry 6, 4f). Yellow solid: ^{1}H NMR (300 MHz, DMSO-

Table 1 Synthesis of 2-amino-4*H*-chromenes in aqueous medium[a]

Entry	Aromatic aldehyde	Time (h)	Yield[b] (%)	TON[c]	Product	Conversion (%)
1	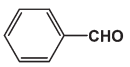	12	86	77	**4a**	95
2	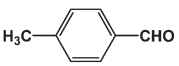	14	80	72	**4b**	92
3	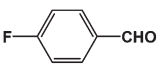	12	82	73	**4c**	90
4	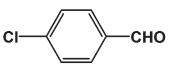	15	80	72	**4d**	92
5	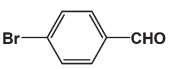	12	83	75	**4e**	92
6	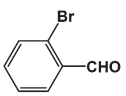	12	79	72	**4f**	88
7	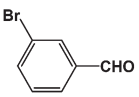	11	81	73	**4g**	90
8	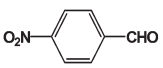	12	85	76	**4h**	95
9	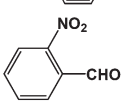	14	78	71	**4i**	86
10	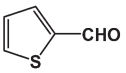	14	77	69	**4j**	86

[a] Reaction conditions: Ar-CHO: 1.0 equiv., resorcinol: 1.0 equiv. (110 mg), malononitrile: 1.0 equiv. (66 mg), solvent: water, reaction temperature: 100 °C (oil bath), catalyst: 30 mg. [b] Isolated yield of pure product. [c] Turn over number (TON) = moles of substrate converted per mole of active site.

d_6) δ 9.75 (b, 1H), 7.56–7.60 (m, 1H), 7.30–7.36 (m, 1H), 7.12–7.18 (m, 2H), 6.91 (s, 1H), 6.71–6.74 (d, 1H, J = 9 Hz), 6.44–6.49 (m, 1H), 6.40–6.41 (m, 1H), 5.14 (s, 1H); ^{13}C NMR (300 MHz, DMSO-d_6) δ 55.14, 79.14, 102.28, 112.53, 120.15, 122.27, 128.45, 128.81, 129.10, 130.97, 132.82, 144.55, 148.86, 157.36, 158.42, 160.38.

2-Amino-3-cyano-7-hydroxy-4-(3-bromophenyl)-4*H*-chromene (Table 1, entry 7, 4g). Yellow solid: ^{1}H NMR (500 MHz, DMSO-d_6) δ 9.74 (s, 1H), 7.40–7.42 (d, 1H, J = 10 Hz), 7.34 (s, 1H), 7.27–7.30 (t, 1H), 7.17–7.19 (d, 1H, J = 10 Hz), 6.93 (s, 2H), 6.81–6.83 (d, 1H, J = 10 Hz), 6.49–6.52 (m, 1H), 6.415–6.419 (d, 1H, J = 2 Hz), 4.68 (s, 1H); ^{13}C NMR (500 MHz, DMSO-d_6) δ 56.33, 102.91, 113.17, 113.60, 121.03, 122.43, 127.18, 130.21, 130.49, 130.58, 131.52, 149.45, 149.71, 157.91, 160.98.

2-Amino-3-cyano-7-hydroxy-4-(4-nitrophenyl)-4*H*-chromene (Table 1, entry 8, 4h). Chocolate colour solid: ^{1}H NMR (500 MHz, DMSO-d_6) δ 9.80 (b, 1H), 8.29–8.31 (m, 2H), 7.44–7.46 (d, 2H), 7.02 (s, 2H), 6.79–6.81 (d, 1H), 6.44–6.53 (m, 2H), 4.86 (s, 1H); ^{13}C NMR (500 MHz, DMSO-d_6) δ 55.34, 79.62, 102.89, 112.82, 113.11, 118.66, 120.74, 124.44, 129.17, 130.39, 146.80, 154.20, 157.99, 160.90.

2-Amino-3-cyano-7-hydroxy-4-(2-nitrophenyl)-4*H*-chromene (Table 1, entry 9, 4i). Chocolate colour solid: ^{1}H NMR (300 MHz, DMSO-d_6) δ 9.97 (s, 1H), 8.66–8.68 (m, 1H), 8.45–8.48 (m, 1H), 8.27–8.30 (m, 1H), 8.11–8.12 (m, 1H), 7.82 (s, 2H), 7.71–7.74 (m, 1H), 7.59–7.61 (m, 1H), 7.27–7.33 (m, 1H), 5.97 (s, 1H); ^{13}C NMR (300 MHz, DMSO-d_6) δ 55.82, 103.02, 106.78, 112.52, 113.32, 120.63, 124.31, 128.79, 130.20, 132.00, 134.06, 140.00, 149.36, 158.19, 159.04, 160.97.

2-Amino-3-cyano-7-hydroxy-4-(thiophenyl)-4*H*-chromene (Table 1, entry 10, 4j). Chocolate colour solid: ^{1}H NMR (300 MHz, DMSO-d_6) δ 9.74 (s, 1H), 7.33–7.35 (m, 1H), 6.86–6.97 (m, 3H), 6.50–6.54 (m, 1H), 6.38 (s, 2H), 6.15–6.18 (m, 1H), 4.97 (s, 1H); ^{13}C NMR (300 MHz, DMSO-d_6) δ 56.50, 102.21, 106.21, 112.42, 113.54, 120.50, 124.02, 126.75, 129.86, 148.56, 151.49, 157.34, 158.44, 160.34.

Results and discussion

The small angle powder X-ray diffraction (PXRD) patterns of 3-chloropropyl functionalized SBA-15 (SBA-15-Cl) and tungstic acid-functionalized mesoporous SBA-15 (TAFMC-1) are shown in the Fig. 1. As seen in Fig. 1a SBA-15-Cl displays three characteristic peaks at the 2θ values of 1.00, 1.69 and 1.93, which could be attributed for the 100 (strong), 110 (weak) and 200 (weak) reflections respectively, corresponding to the 2D-hexagonal mesostructure. When SBA-15-Cl was functionalized with tungstic acid then a considerable decrease in the intensity and shift in peak positions are observed, however 2D-hexagonal ordering has been retained (Fig. 1b). This decrease in the intensities of the peaks reveals that tungstic acid has been successfully incorporated at the surface of the functionalized mesoporous SBA-15 material.[20]

N_2 adsorption/desorption isotherms of the tungstic acid-functionalized TAFMC-1 at 77 K is shown in the Fig. 2. The

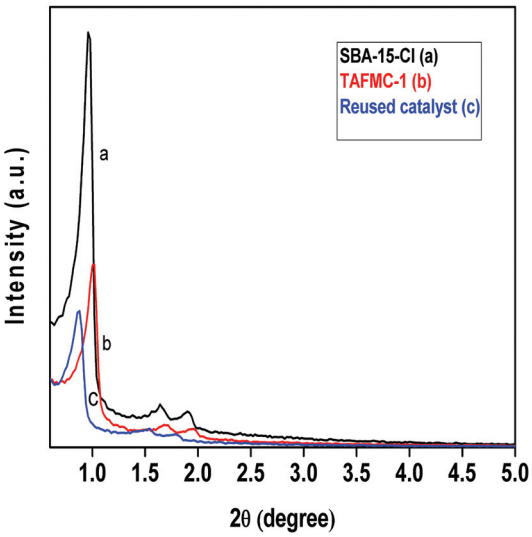

Fig. 1 Small angle powder XRD pattern of SBA-15-Cl (a), tungstic acid functionalized SBA-15 (b), TAFMC-1 mesoporous catalyst after using six times (c).

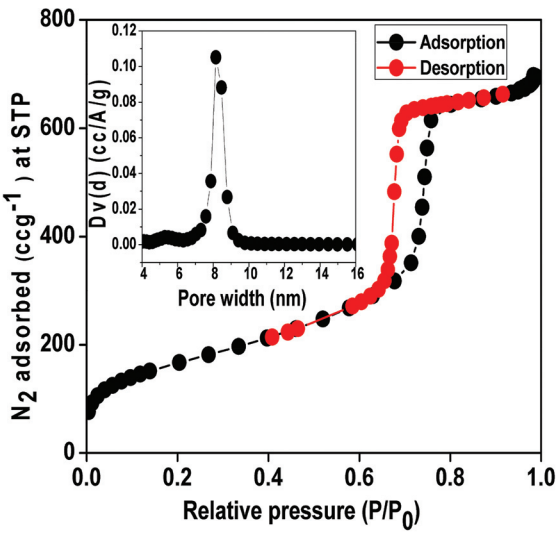

Fig. 2 N_2 adsorption/desorption isotherm of the mesoporous catalyst TAFMC-1 at 77 K temperature. Pore size distributions estimated through NLDFT method is shown in the inset.

sample shows a typical type IV isotherm with a very large hysteresis loop in the 0.6 to 0.8 P/P_0 of N_2. The BET surface areas for the pure 3-chloropropyl functionalized mesoporous SBA-15 and TAFMC-1 are 680 m^2 g^{-1} and 590 m^2 g^{-1}, respectively. A considerable decrease in the BET surface area upon covalent grafting of tungstic acid at the surface of 3-chloropropyl-functionalized SBA-15 material suggests that tungstic acid groups have been anchored at the surface of mesopores.[21] The pore size distribution of the TAFMC-1 has been evaluated by employing non-local density functional theory (NLDFT) shown in the inset of Fig. 2 suggests that uniform distribution of large mesopores throughout the sample with the pore dimensions *ca.* 8.1 nm. The pore dimension for the SBA-15-Cl

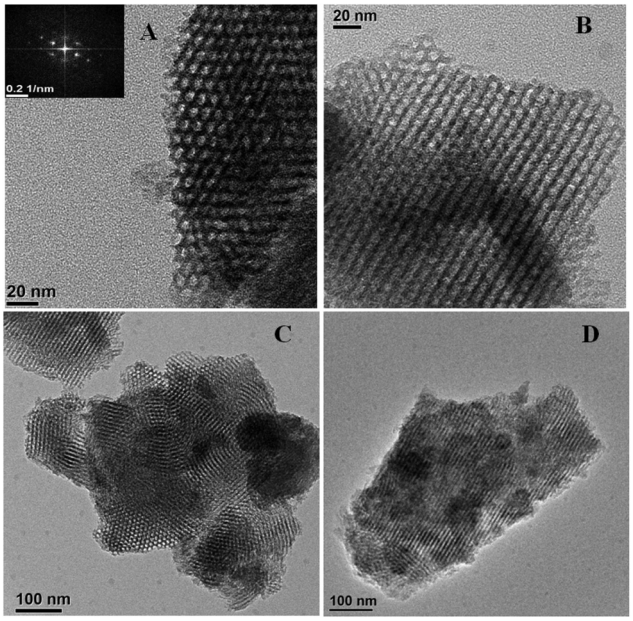

Fig. 3 HR TEM images of TAFMC-1 (A, parallel to pore axis, FFT pattern is shown in the inset), (B, perpendicular to pore axis), HR TEM images of TAFMC-1 after using four times (C, parallel to pore axis), (D, perpendicular to pore axis).

material was 9.6 nm, which has been distinctly reduced to 8.1 nm after grafting of tungstic acid. The considerable decrease in the pore dimension clearly suggests that tungstic acid molecule has been anchored into the pore channel of the mesoporous SBA-15-Cl material. Calculated pore volume of TAFMC-1 is 1.024 cc g^{-1}, which is considerably large. This together with the pore width of 8.1 nm is good enough to carry out the one-pot three component condensation reaction over TAFMC-1.

The HR TEM images of TAFMC-1 are shown in Fig. 3. This electron microscopic image clearly suggests that uniformly ordered mesopores of dimensions *ca.* 7.2–7.5 nm have been arranged in a honeycomb like hexagonal array throughout the sample. The FFT diffractogram shown in the inset of Fig. 3 further suggests 2D-hexagonal pore channels. The TEM image (Fig. 3B perpendicular to the pore axis) also illustrates that the channel directions are parallel to the thickness of the plate, and the 110 reflection plane of the sample is clearly viewed in this image. From these TEM images we can conclude that the TAFMC-1 has ordered mesopores with a 2D-hexagonal structure and the hexagonally ordered mesoporous structure of SBA-15 is preserved after tungstic acid functionalization.[22]

In order to evaluate incorporation of organic groups and tungsten moieties into the pore channel of SBA-15, FT-IR spectra of the respective SBA-15-Cl and TAFMC-1 have been analyzed. The FT-IR spectra of sodium tungstate dihydrate, SBA-15-Cl, TAFMC-1 and reused catalyst are shown in Fig. 4. The absorptions at 3439, 2978, 1631, 1080, 966, 799, 573, 475 cm^{-1} appear in the TAFMC-1 indicates the presence of chloropropyl and WO_4 groups. An absorbance at 2978 cm^{-1}, could be assigned to the methylene stretching vibrations of the propyl chain of organosilane moiety. This data clearly

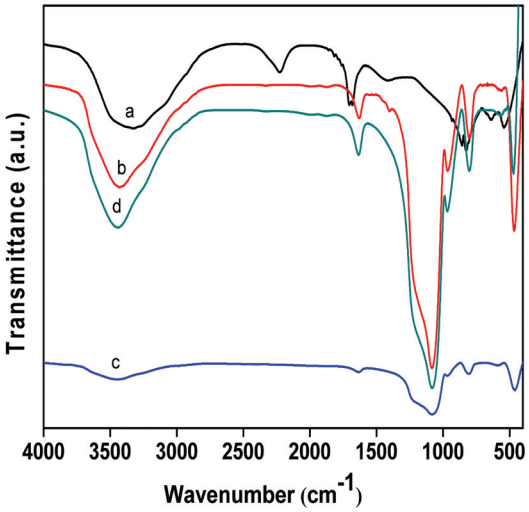

Fig. 4 FTIR spectra of $Na_2WO_4{\cdot}2H_2O$ (a), reused catalyst (b), SBA-15-Cl (c), and mesoporous catalyst TAFMC-1 (d).

indicates incorporation of 3-chloropropyl organic moiety in the pore channel of SBA-15. The FT-IR spectra of TAFMC-1 displays a peak at 966 cm^{-1}, which could be attributed to the stretching vibration of W=O.[23] The peak centered at 1041 cm^{-1}, corresponding to the bending vibration of W–OH, cannot be resolved due to the overlap with the absorbance of the Si–O–Si stretch in the 1000–1246 cm^{-1} range. The peak appeared in the range of 3439 cm^{-1} can be assigned to the hydroxyl stretching of the hydrogen bonded internal silanol groups. The characteristic bands of SiO_2 related to the Si–O stretching vibrations appeared at *ca.* 1080 and 799 cm^{-1}. The bending vibrations of the surface silanols and Si–O unit can be recognized by the presence of the bands at 950 and 475 cm^{-1}, respectively. FE SEM image (Fig. 5) of the mesoporous catalyst TAFMC-1 illustrates irregular particle morphology of the catalyst.

Solid state ^{13}C CP MAS and ^{29}Si MAS NMR data provides the information about the chemical environment around C and Si in the hybrid frameworks of the mesoporous catalyst TAFMC-1. In ^{13}C CP MAS NMR (shown in Fig. 6), there are three peaks with chemical shift at 12.6 ppm, 29.2 ppm and 50.5 ppm respectively, indicating the presence of three types of carbon. These characteristic signals can be attributed to the aliphatic propyl group attached with the Si, C3, C2 and C1 respectively (Fig. 6). ^{29}Si MAS NMR spectrum of TAFMC-1 catalyst (Fig. 7) exhibits three broad peaks with chemical shift at −92.107 ppm, −101.520 ppm and −111.143 ppm, which could be attributed to the T^3 [C-Si$(OSi)_3$], Q^3 [$(SiO)_3$Si(OH)], Q^4 [Si$(OSi)_4$] species respectively.[24] These spectroscopic results suggest that the organic propyl moiety incorporated in the hybrid silica framework.

Titrimetric estimation of –OWO_3H group loading

We have calculated the loading of –OWO_3H group in the framework of TAFMC-1 by a back titration method adding a

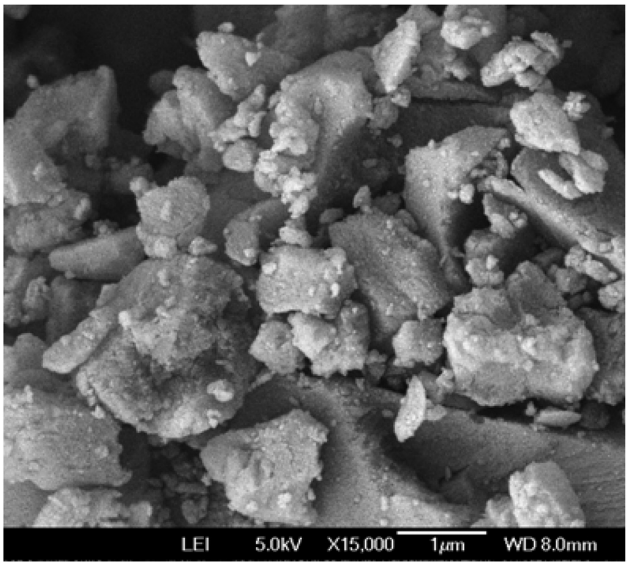

Fig. 5 FE SEM image of the catalyst TAFMC-1.

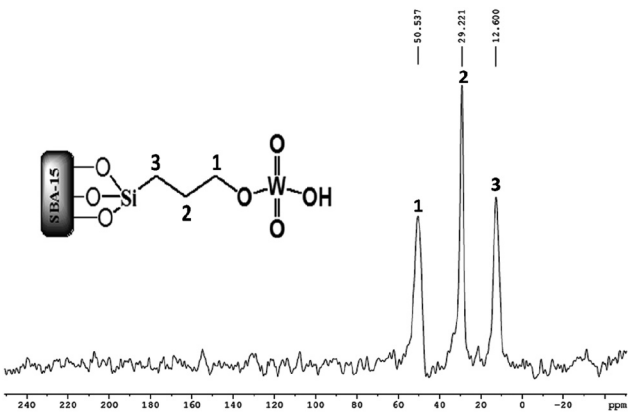

Fig. 6 ^{13}C CP-MAS NMR spectrum of the catalyst TAFMC-1.

known strength of NaOH solution. It is assumed that all $-OWO_3H$ groups would be replaced by $-OWO_3^-Na^+$ during NaOH treatment. The excess NaOH was back titrated with a known strength of oxalic acid. The strength of NaOH solution was kept very low (0.01 N) in order to avoid the consumption of the base in the hydrolysis of the mesoporous silica frameworks. This titrimetric experimental data suggests that 1 g TAFMC-1 catalyst contains 0.37 mmol $-OWO_3H$ groups.

Catalysis

Effect of the amount of catalyst. It was found that the condensation reaction among aromatic aldehyde (**1**), malononitrile (**2**) and resorcinol (**3**) produces 2-amino-4*H*-chromenes (**4**) in the presence of mesoporous TAFMC-1 catalyst in aqueous medium under refluxing conditions (Scheme 2). When the reaction was carried out in the absence of any catalyst no product was formed. In order to evaluate the optimum amount of catalyst required for the one-pot three component condensation reaction, the reaction was carried out in the

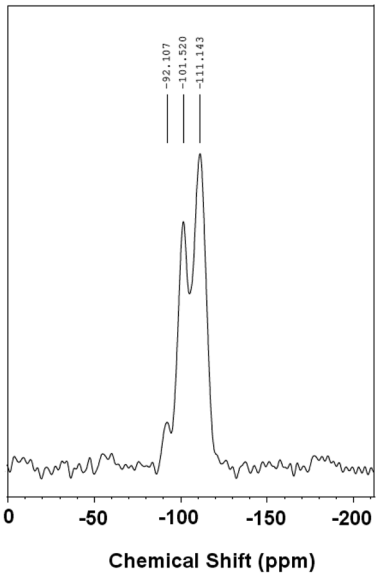

Fig. 7 ^{29}Si MAS NMR spectrum of the catalyst TAFMC-1.

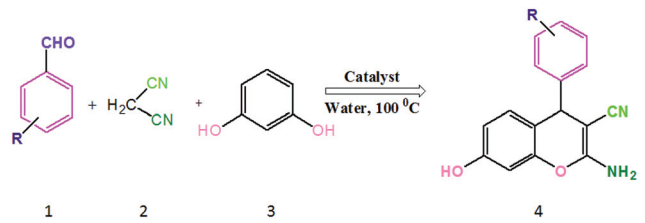

Scheme 2

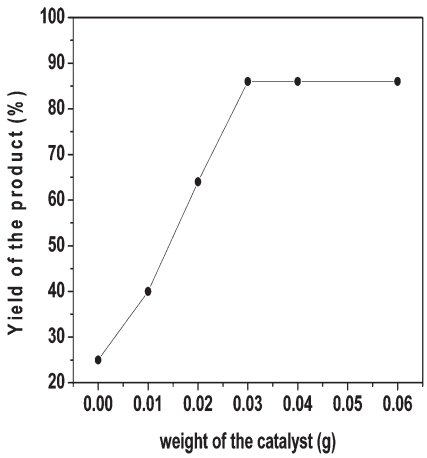

Fig. 8 Effect of the catalyst loading in one-pot three component condensation reaction.

presence of varying amounts of catalyst from 0.01 g to 0.06 g in aqueous medium under refluxing conditions (Fig. 8). From Fig. 8 we can conclude that 0.03 g of TAFMC-1 is the optimum amount of catalyst needed to conduct this condensation reaction. When the amount of catalyst has been increased more to perform this catalytic reaction no further increase of product

Table 2 Effect of the solvent in the TAFMC-1 catalyzed condensation of resorcinol, malononitrile, and benzaldehyde

Solvent	Yield[a,b]
Water	86
Acetonitrile	23
Methanol	75
Ethanol	78
DMF	15
THF	12
DCM	10
Solvent-free	30
n-Hexane	8

[a] All the reactions were carried out under reflux condition. Reaction condition: Ph-CHO: 1.0 equiv. (106 mg), resorcinol: 1.0 equiv. (110 mg), malononitrile: 1.0 equiv. (66 mg). Solvent-free reaction was carried out at 100 °C. [b] Isolated yields.

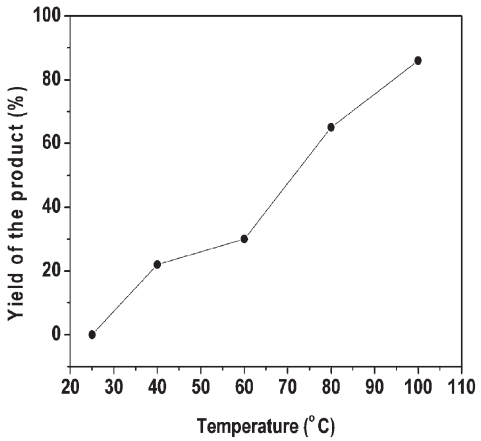

Fig. 9 Effect of reaction temperature for the one-pot three component condensation reaction.

yield has been observed. On the other hand, the product yield and the rate of condensation reaction is decreased with decreasing amount of catalyst compared to that required for the optimum amount of catalyst.

Effect of solvent. To determine the best reaction conditions, we have carried out the condensation of benzaldehyde, malononitrile and resorcinol over TAFMC-1 in the presence of various solvents such as water, acetonitrile, methanol, ethanol, DMF, THF, DCM, *n*-hexane under refluxing conditions (Table 2). For solvents like acetonitrile, DMF, THF, DCM and *n*-hexane Knoevenagel condensation adduct was formed as a major product and the desired product was formed only in 23%, 15%, 12%, 10% and 8% yields, respectively. But when the reaction was carried out in polar protic solvents such as water, methanol, ethanol, yield of the desired product was increased to 86%, 75% and 78%, respectively. Here the product is more polar than the reactants so when we have used polar protic solvents the yield of the products was increased. The fate of reaction was also investigated under solvent-free conditions. But under this condition only a small amount of the desired product was obtained, which indicates that water is the optimum solvent for the completion of this one-pot three component condensation reaction.

Effect of the reaction temperature. The activity of catalyst TAFMC-1 for the synthesis of the chromene derivatives in aqueous medium increases with increasing temperature. The effect of reaction temperature has been investigated in the condensation reaction of benzaldehyde, malononitrile and resorcinol under aqueous medium at different temperatures (Fig. 9). When the reaction was performed at room temperature (25 °C) for 24 h in aqueous medium, no product was found. As the temperature of the reaction was increased to 40 °C, the yield of the product was 22%. Further, we performed the reaction at three different temperatures such as 60, 80 and 100 °C. From the activity profile shown in Fig. 9 it is clear that the yield of the product is a maximum 86% at 100 °C.

Control experiment for the three component condensation reaction. In order to understand the nature of bonding of tungsten with the organically functionalized mesoporous

Table 3 Screening of the different catalysts for the synthesis of 2-amino-4*H*-chromenes[a]

Entry	Catalyst	Temperature (°C)	Solvent	Yield (%)
1	No catalyst	25	None	0
2	No catalyst	25	Water	0
3	No catalyst	50	Water	0
4	No catalyst	100	Water	8
5	$FeCl_3$	100	Water	18
6	$AlCl_3{\cdot}6H_2O$	100	Water	12
7	SBA-15	100	Water	5
8	SBA-15-Cl	100	Water	5
9	SBA-15-Cl with aqueous HCl	100	Water	12
10	$Na_2WO_4{\cdot}2H_2O$	100	Water	45
11	H_2WO_4	100	Water	40
12	TAFMC-1	100	Water	80

[a] Reaction condition: 4-chlorobenzaldehyde (1 mmol, 140 mg), resorcinol (1 mmol, 110 mg), malononitrile (1 mmol, 66 mg), solvent free or solvent (water, 5 mL), catalyst (30 mg).

SBA-15, a control experiment for this condensation reaction has been performed in the absence of any catalyst. The condensation reaction was carried out at different temperatures under solvent-free or aqueous medium in the absence of any catalyst (Table 3, entries 1–3). Under this condition no yield corresponding to the expected condensation product has been observed and starting materials remain unreacted. When the condensation reaction was performed at 100 °C temperature in the absence of any catalyst then only 8% product yield was obtained (Table 3, entry 4). This yield could be due to the higher reaction temperature where thermal condensation reaction becomes more facile. We have employed various homogeneous Lewis acid catalysts like $FeCl_3$ or $AlCl_3{\cdot}6H_2O$ in order to compare the catalytic activity of TAFMC-1. But very poor yields of the product were obtained (Table 3, entries 5 and 6). In the presence of SBA-15 and SBA-15-Cl only very small amounts of the products are generated in aqueous medium at 100 °C temperature (Table 3, entries 7 and 8). Then the condensation reaction was conducted by employing SBA-15-Cl in

the presence of aqueous HCl (Table 3, entry 9). A small increase in the product yield is observed which may be due to the presence of aqueous HCl. Homogeneous phase $Na_2WO_4{\cdot}2H_2O$ (Table 3, entry 10) has been utilized as the catalyst for carrying out this condensation reaction. Only 45% yield of the corresponding product has been obtained. The reaction has also been carried out in the presence of H_2WO_4 catalyst (Table 3, entry 11). But no appreciable increase in the product yield has been obtained. When our mesoporous heterogeneous catalyst TAFMC-1 has been employed for this condensation reaction then the yield of the product was dramatically increased to 80% (Table 3, entry 12). This result clearly suggests that the mesoporosity plays a significant role in this condensation reaction. The surface area and pore size for this mesoporous TAFMC-1 catalyst is large enough to allow the diffusion of large organic molecules and helps them to interact with each other for performing this one-pot three component condensation reaction. Aromatic aldehydes attached with both electron-withdrawing and electron donating groups participated in the one-pot three component condensation reaction very smoothly with very good efficiency (Table 1, see the NMR data in the Experimental section). Thus, the nature and position of substituted groups present in the aromatic ring do not show any pronounced effect on the reaction. The condensation reaction was performed for the both *meta*-substituted aromatic aldehyde (Table 1, entry 7) and as well as heteroaromatic aldehyde such thiophene-2-carbaldehyde (Table 1, entry 10) without any difficulty. Several sensitive functional groups such as –Cl, –Br and $-NO_2$ attached to the aromatic ring are also compatible for this reaction. The turn over numbers (TONs) for the different reactions vary for different aldehydes, suggesting high catalytic activity of TAFMC-1 generated from the tungsten species incorporated into the porous channel of organically functionalized SBA-15. All the conversions of the products (%) are listed in Table 1. The condensation reaction was also performed with different active methylene compounds, such as malononitrile, ethyl cyanoacetate and diethyl malonate in the presence of the TAFMC-1 catalyst in aqueous medium using benzaldehyde and resorcinol as the representative case. Malononitrile has been considered as the best suited active methylene compound to conduct this one-pot three component condensation reaction as the highest yield of the desired product has been obtained in this case. The W content in the fresh catalyst is 0.0019 mmol g^{-1}, as measured by ICP-OES analysis.

Reusability of the catalyst

The reusability of the mesoporous TAFMC-1 in the one-pot three component condensation reaction was examined using benzaldehyde, malononitrile and resorcinol as reference. After completion of the reaction, the catalyst was separated from the reaction mixture by filtration, washed with dichloromethane followed by diethyl ether. Then the recovered catalyst was dried at room temperature for 12 h and heated in the oven at 75 °C for activation of the catalyst. After recovery of the catalyst it has been employed for a further six additional repetitive reaction cycles. In all cases, consistent catalytic activity over mesoporous TAFMC-1 has been observed, establishing the fact that the catalyst can be recycled and reused without any considerable loss of catalytic activity (Table 4). A very small amount of product has been observed, which could be attributed to the loss of catalyst recovery during the course of reaction.

Table 4 Recycling potential of mesoporous catalyst TAFMC-1 in the one-pot three component condensation reaction

No. of cycles[a]	Fresh	Run 1	Run 2	Run 3	Run 4	Run 5
Yield[b] (%)	86.0	86.0	84.0	84.0	84.0	82.0
Time (h)	12.0	12.0	12.0	12.0	12.0	12.0
TON[c]	77	76	76	75	75	74

[a] Reaction condition: benzaldehyde = 1.0 equiv. (106 mg), resorcinol = 1.0 equiv. (110 mg), malononitrile = 1.0 equiv. (66 mg), aqueous medium at 100 °C temperature. [b] Isolated yield of product. [c] Turn over number = moles of substrate converted per mole of active site.

Leaching test

In order to check any leaching of metal from the solid catalyst we have performed an *in situ* filtration technique. In this technique the catalyst (0.03 g) was stirred in 5 mL water for 24 h at 100 °C temperature, after filtration the filtrate was taken in a 50 mL round bottom flask and it was evaporated to dryness. Then 1.0 mmol of each of the benzaldehyde, resorcinol and malononitrile were taken in the same round bottom flask in aqueous medium at 100 °C for 12 h. However, in this case no product was found, suggesting that no leaching of the tungsten metal occurred before the filtration.

Hot filtration test

Furthermore, in order to check any leaching of W metal into the solution during the reaction, a hot-filtration test was performed with TAFMC-1 for the condensation reaction. In such technique, benzaldehyde (1 mmol, 106 mg) was allowed to react with resorcinol (1 mmol, 110 mg) and malononitrile (1 mmol, 66 mg) in aqueous medium with 0.03 g catalyst. The reaction was performed at 100 °C and after 6 h under hot conditions the reaction mixture was immediately filtered. At this stage the yield of the product was 52% (confirmed by ^{1}H NMR). After that the reaction was continued for a further 6 h at the same temperature as the filtrate. However, no increase of the product yield beyond 52% was observed after 12 h reaction time. This result clearly confirms the heterogeneous nature of the mesoporous catalyst TAFMC-1 and no leaching of W metal occurs during the course of reaction. ICP-OES analysis has also been performed for the reused catalyst after the six repetitive catalytic reaction cycles. After the six reaction cycle the W content was marginally decreased to 0.0016 mmol g^{-1} (this decrease is within the experimental error of chemical analysis). This data clearly revealed the fact that the tungsten metal has been covalently bonded with the organic groups present in the mesoporous channel of the catalyst and the catalytic reactions are purely heterogeneous in nature.

Characterization of reused catalyst

The reused TAFMC-1 catalyst was further characterized by small angle powder XRD, TEM, FT-IR studies in order to investigate if any further change takes place in the catalyst after reaction. Small angle powder XRD pattern of the reused mesoporous catalyst displays (Fig. 1) a characteristic mesophase, which clearly reveals that the hexagonal mesostructure of the reused catalyst are carefully preserved during the course of the catalytic reaction. In Fig. 1c it is quite evident that a small shift in the peak position for the reused catalyst is observed. After six repetitive reaction cycles the expansion in pore-wall for the reused catalyst could occur due to the hydrolysis of silica species present at the catalyst surface. As a result *d*-spacing for the reused catalyst is increased. This increase in the *d*-spacing is responsible for the shift in the peak position for the reused catalyst. The TEM images of the reused heterogeneous catalyst after the fourth catalytic cycle suggest that the ordered mesostructure of the reused catalyst remains unaffected after the reaction (Fig. 3). We took the FT-IR spectra of the catalyst after the sixth catalytic cycle (Fig. 4), where the strong absorption band at 966 cm^{-1} is observed, which corresponds to the presence of W=O bond after use of the catalyst. The above results revealed that the mesoporous heterogeneous catalyst was very stable during the one-pot three component condensation reaction.

Plausible reaction pathway. The possible reaction pathway for the synthesis of 2-amino-4*H*-chromenes using mesoporous catalyst having an acidic site involved the Knoevenagel condensation reaction between aromatic aldehyde and malononitrile at the first step, then Michael addition occurred between the Knoevenagel product and resorcinol, which is followed by intra-molecular cyclization to yield 2-amino-4*H*-chromenes. Here W(VI) increases the electrophilicity of the aldehydic carbon atom followed by dehydration to give the Knoevenagel product.[25] Again W(VI) increases the electrophilicity of –CN group so that Michael addition can occur and followed by intra-molecular cyclization and tautomerization to yield the 2-amino-4*H*-chromene derivatives.[19,26]

Conclusions

From the above experimental results we can conclude that a novel tungstic acid functionalized highly ordered 2D-hexagonal mesoporous material can be designed through post-synthetic functionalization *via* a 3-chloropropyl group. This mesoporous catalyst showed good surface area and acidity and thus can be utilized very efficiently for the one-pot three component condensation reaction of aromatic aldehyde, malononitrile and resorcinol in aqueous medium for the synthesis of 2-amino-4*H*-chromenes. Thus, tungstic acid functionalized mesoporous material may find potential utility in the environment friendly liquid phase acid catalytic reactions by using water as solvent.

Acknowledgements

SKK and JM thank CSIR, New Delhi for their respective junior and senior research fellowships. This work is partly funded by DST Unit on Nanoscience.

References

1 M. M. Heravi, B. Baghernejad and H. A. Oskooie, *J. Chin. Chem. Soc.*, 2008, **55**, 659–662.
2 N. Hall, *Science*, 1994, **266**, 32–34.
3 (*a*) M. R. Naimi-Jamal, S. Mashkouri and A. Sharifi, *Mol. Divers.*, 2010, **14**, 473–477; (*b*) A. Kumar, S. Sharma, R. A. Maurya and J. Sarkar, *J. Comb. Chem.*, 2010, **12**, 20–24.
4 M. M. Khafagy, A. H. F. A. El-Wahas, F. A. Eid and A. M. El-Agrody, *Farmaco*, 2002, **57**, 715–722.
5 K. Hiramoto, A. Nasuhara, K. Michiloshi, T. Kato and K. Kikugawa, *Mutat. Res.*, 1997, **395**, 47–56.
6 M. Kidwai, S. Saxena, M. K. R. Khan and S. S. Thukral, *Bioorg. Med. Chem. Lett.*, 2005, **15**, 4295–4298.
7 (*a*) A. G. Martinez and L. J. Marco, *Bioorg. Med. Chem. Lett.*, 1997, **7**, 3165–3170; (*b*) W. P. Smith, L. S. Sollis, D. P. Howes, C. P. Cherry, D. I. Starkey and N. K. Cobley, *J. Med. Chem.*, 1998, **41**, 787–797.
8 S. J. Mohr, M. A. Chirigos, F. S. Fuhrman and J. W. Pryor, *Cancer Res.*, 1975, **35**, 3750–3754.
9 C. S. Konkoy, D. B. Fisck, S. X. Cai, N. C. Lan and J. F. W. Keana, *PCT Int. Appl* WO 0075123, 2000; *Chem. Abstr.*, 2001, **134**, 29313a.
10 (*a*) G. P. Ellis, in *The Chemistry of Heterocyclic Compounds. Chromenes, Chromanes and Chromones*, ed. A. Weissberger and E. C. Taylor, John Wiley, New York, 1977, ch. 11, p. 11; (*b*) E. A. Hafez, M. H. Elnagdi, A. G. A. Elagemey and F. M. A. A. El-Taweel, *Heterocycles*, 1987, **26**, 903–907; (*c*) M. A. Sofan, F. M. A. A. El-Taweel and M. H. Elnagdi, *Liebigs Ann. Chem.*, 1989, 935–936; (*d*) F. M. Abdel Galil, B. Y. Riad, S. M. Sherif and M. H. Elnagdi, *Chem. Lett.*, 1982, 1123–1126.
11 A.-Q. Zhang, M. Zhang, H.-H. Chen, J. Chen and H.-Y. Chen, *Synth. Commun.*, 2007, **37**, 231–235.
12 Y. Ren and C. Cai, *Catal. Commun.*, 2008, **9**, 1017–1020.
13 D. Kumar, V. B. Reddy, B. G. Mishra, R. K. Rana, M. N. Nadagaouda and R. S. Varma, *Tetrahedron*, 2007, **63**, 3093–3097.
14 B. S. Kumar, N. Srinivasulu, R. H. Udupi, B. Rajitha, Y. T. Reddy, P. N. Reddy and P. S. Kumar, *J. Heterocycl. Chem.*, 2006, **43**, 1691–1693.
15 G. Shanthi and P. T. Perumal, *Tetrahedron Lett.*, 2007, **48**, 6785–6789.
16 A. Shaabani, R. Ghadari, S. Ghasemi, M. Pedarpour, A. H. Rezayan, A. Sarvary and S. Weng Ng, *J. Comb. Chem.*, 2009, **11**, 956–959.
17 (*a*) A. Dutta, J. Mondal, A. K. Patra and A. Bhaumik, *Chem.–Eur. J.*, 2012, **18**, 13372–13378; (*b*) A. Modak, J. Mondal, V. K. Aswal and A. Bhaumik, *J. Mater. Chem.*, 2010, **20**,

8099–8106; (*c*) J. Mondal, A. Modak, A. Dutta and A. Bhaumik, *Dalton Trans.*, 2011, **40**, 5228–5235.

18 (*a*) A. Modak, J. Mondal and A. Bhaumik, *Green Chem.*, 2012, **14**, 2840–2855; (*b*) J. Mondal, A. Modak, A. Dutta, S. Basu, S. N. Jha, D. Bhattacharyya and A. Bhaumik, *Chem. Commun.*, 2012, **48**, 8000–8002; (*c*) C. Perego and R. Millini, *Chem. Soc. Rev.*, 2013, **42**, 3956–3976.

19 J. Mondal, A. Modak, M. Nandi, H. Uyama and A. Bhaumik, *RSC Adv.*, 2012, **2**, 11306–11317.

20 J. Mondal, T. Sen and A. Bhaumik, *Dalton Trans.*, 2012, **41**, 6173–6181.

21 (*a*) M. Nandi, J. Mondal, K. Sarkar, Y. Yamauchi and A. Bhaumik, *Chem. Commun.*, 2011, **47**, 6677–6679; (*b*) S. L. Jain, A. Modak and A. Bhaumik, *Green Chem.*, 2011, **13**, 586–590.

22 (*a*) J. Mondal, M. Nandi, A. Modak and A. Bhaumik, *J. Mol. Catal. A: Chem.*, 2012, **363–364**, 254–264; (*b*) B. Karimi, A. Biglari, J. H. Clark and V. Budarin, *Angew. Chem., Int. Ed.*, 2007, **46**, 7210–7213; (*c*) J. Balamurugan, R. Thangamuthu and A. Pandurangan, *J. Mater. Chem. A*, 2013, **1**, 5070–5080.

23 (*a*) S. Khodabakhshi and B. Karami, *Catal. Sci. Technol.*, 2012, **2**, 1940–1944; (*b*) J. Pfeifer, C. Guifang, P. Tekula-Buxbaum, B. A. Kiss, M. Farkas-Jahnke and K. Vadasdi, *J. Solid State Chem.*, 1995, **119**, 90–97.

24 (*a*) A. Monge-Marcet, X. Cattoën, D. A. Alonso, C. Nájera, M. W. C. Manb and R. Pleixats, *Green Chem.*, 2012, **14**, 1601–1610; (*b*) S.-Y. Chen, T. Yokoi, C.-Y. Tang, L.-Y. Jang, T. Tatsumi, J. C. C. Chan and S. Cheng, *Green Chem.*, 2011, **13**, 2920–2930; (*c*) Y.-J. Li, B. Yan and L. Wang, *Dalton Trans.*, 2011, **40**, 6722–6731.

25 J. Juan-Alcaniz, E. V. Ramos-Fernandez, U. Lafont, J. Gascon and F. Kapteijn, *J. Catal.*, 2010, **269**, 229–241.

26 S. Makarem, A. A. Mohammadi and A. R. Fakhari, *Tetrahedron Lett.*, 2008, **49**, 7194–7196.

